

Anthropogenic emissions of highly reactive volatile organic compounds in eastern Texas inferred from oversampling of satellite (OMI) measurements of HCHO columns

Lei Zhu¹, Daniel J Jacob¹, Loretta J Mickley¹, Eloïse A Marais¹, Daniel S Cohan², Yasuko Yoshida³, Bryan N Duncan⁴, Gonzalo González Abad⁵ and Kelly V Chance⁵

¹ School of Engineering and Applied Sciences, Harvard University, Cambridge, MA, USA

² Civil and Environmental Engineering, Rice University, Houston, TX, USA

³ Science Systems and Applications, Inc., Lanham, MD, USA and NASA Goddard Space Flight Center, Greenbelt, MD, USA

⁴ NASA Goddard Space Flight Center, Greenbelt, MD, USA

⁵ Harvard-Smithsonian Center for Astrophysics, Cambridge, MA, USA

E-mail: leizhu@fas.harvard.edu

Received 12 June 2014, revised 7 October 2014

Accepted for publication 8 October 2014

Published 3 November 2014

Abstract

Satellite observations of formaldehyde (HCHO) columns provide top-down constraints on emissions of highly reactive volatile organic compounds (HRVOCs). This approach has been used previously in the US to estimate isoprene emissions from vegetation, but application to anthropogenic emissions has been stymied by lack of a discernable HCHO signal. Here we show that temporal oversampling of HCHO data from the Ozone Monitoring Instrument (OMI) for 2005–2008 enables detection of urban and industrial plumes in eastern Texas including Houston, Port Arthur, and Dallas/Fort Worth. By spatially integrating the HCHO enhancement in the Houston plume observed by OMI we estimate an anthropogenic HCHO source of $250 \pm 140 \text{ kmol h}^{-1}$. This implies that anthropogenic HRVOC emissions in Houston are 4.8 ± 2.7 times higher than reported by the US Environmental Protection Agency inventory, and is consistent with field studies identifying large ethene and propene emissions from petrochemical industrial sources.

Keywords: HCHO, ozone monitoring instrument, anthropogenic, highly reactive VOC, oversampling

1. Introduction

Anthropogenic highly reactive volatile organic compounds (AHRVOCs) with atmospheric lifetimes of less than a day are important precursors of ozone and organic aerosols in urban air and industrial plumes. Their sources are poorly quantified

in emission inventories, as shown by air quality studies in eastern Texas (Ryerson *et al* 2003, Parrish *et al* 2012) and in an oil/gas field of northern Colorado (Gilman *et al* 2013). Satellite column measurements of formaldehyde (HCHO), a high-yield product from atmospheric oxidation of VOCs, have been used to constrain AHRVOC emissions in East Asia (Fu *et al* 2007) and Nigeria (Marais *et al* 2014a). However, detection of AHRVOC emissions in the US from satellite HCHO data has been elusive (Martin *et al* 2004, Millet *et al* 2008). The highest-resolution data are from the Ozone Monitoring Instrument (OMI), which provides daily global



Content from this work may be used under the terms of the Creative Commons Attribution 3.0 licence. Any further distribution of this work must maintain attribution to the author(s) and the title of the work, journal citation and DOI.

coverage of HCHO columns by cross-track scanning with $13 \times 24 \text{ km}^2$ nadir pixel resolution (Levelt *et al* 2006). An analysis of OMI urban data in the US by Boeke *et al* (2011) found only weak HCHO enhancements in the New York and Los Angeles urban cores in summer, and in the Houston urban core in spring and fall.

The difficulty of observing US AHRVOC emissions from space likely reflects their relatively small magnitude. The single-retrieval detection limit for OMI HCHO is $2 \times 10^{16} \text{ molecules cm}^{-2}$ (Millet *et al* 2008), which corresponds to $\sim 4 \text{ ppb}$ HCHO in a 2 km deep boundary layer. HCHO concentrations of $\sim 10 \text{ ppb}$ are commonly observed in urban air and industrial plumes (Wert *et al* 2003, Buzcu Guven and Olaguer *et al* 2011, Lin *et al* 2012, Zheng *et al* 2013) but would be diluted on the scale sampled by the satellite pixels. Temporal averaging of the satellite data greatly improves the detection limit (Boeke *et al* 2011), though quantifying this improvement is difficult as it depends on the random versus systematic character of the retrieval error. The urban signal can also be masked by large regional emissions of isoprene, the dominant biogenic HRVOC contributing to HCHO (Palmer *et al* 2003, Martin *et al* 2004, Boeke *et al* 2011).

Here we demonstrate that quantitative detection of AHRVOC emissions in eastern Texas can be achieved by oversampling of the OMI HCHO data. ‘Oversampling’ refers to temporal averaging of the satellite data on a spatial grid finer than the pixel resolution on the instrument. The technique achieves high signal-to-noise ratio at high spatial resolution by sacrificing temporal resolution, i.e., averaging over a long time period. It takes advantage of the spatial offset and changing geometry (from off-track viewing) of the satellite pixels from day to day. Oversampling of OMI data has been applied previously with success to detection of SO_2 and NO_2 from urban and point sources (de Foy *et al* 2009, Fioletov *et al* 2011, McLinden *et al* 2012, Lu *et al* 2013). We demonstrate here its application to HCHO.

2. Data and methods

OMI is a UV/Vis nadir solar backscatter spectrometer launched in 2004 on the Aura satellite (Levelt *et al* 2006). It achieves daily global coverage with an equator crossing time of 13:38 local time. HCHO slant column densities (SCD) along the solar backscatter optical path are fitted in the spectral window 327.5–356.5 nm (Chance *et al* 2000). We use OMI HCHO Version 2.0 (Collection 3) SCD retrievals for 2005–2008 (http://disc.sci.gsfc.nasa.gov/Aura/data-holdings/OMI/omhcho_v003.shtml) that (1) pass all fitting and statistical quality checks, (2) have a cloud fraction less than 0.3 and solar zenith angle less than 60° , and (3) are not affected by the ‘OMI row anomaly’ (www.knmi.nl/omi/research/product/rowanomaly-background.php). Drift from instrument aging (Marais *et al* 2012) is removed with a linear temporal regression of background SCD over the North Pacific (130° – 125°W , 35° – 40°N).

The air mass factor ($\text{AMF} = \text{SCD}/\text{VCD}$) to convert SCD to vertical column density (VCD, column hereafter) is computed following Palmer *et al* (2001) with the LIDORT radiative transfer model (Spurr *et al* 2001). Satellite viewing geometry, cloud fraction, and cloud centroid pressure are from the OMI data. The AMF calculation requires information on HCHO and aerosol vertical distributions, and these are specified locally from the GEOS-Chem model with $0.5^\circ \times 0.667^\circ$ horizontal resolution over North America (Zhang *et al* 2011). Oversampling uses a higher horizontal resolution for the OMI data than $0.5^\circ \times 0.667^\circ$, but we expect that the error from subgrid variability in the HCHO and aerosol vertical distributions is small relative to other sources of error.

Wintertime observations would avoid biogenic interference on HCHO but we find that OMI HCHO columns are then indistinguishable from noise over the US including over Houston. This does not reflect loss of measurement sensitivity as the mean AMF over Houston in winter (December–February; $\text{AMF} = 0.99 \pm 0.17$) is actually higher than in summer (May–August; $\text{AMF} = 0.78 \pm 0.13$). The higher AMF in winter is due to longer light path and lower cloud cover, more than compensating for the effects of reduced UV light penetration and shallower planetary boundary layer (PBL). We attribute the lack of detectable HCHO in winter to low OH concentrations, delaying the oxidation of AHRVOCs to HCHO and thus smearing the HCHO signal. Average 12:00–15:00 (local time) OH concentrations in the GEOS-Chem model over Houston are a factor of 5 lower in December–February than in May–August. Mean surface wind speeds are 30% higher in December–February than May–August (www.wunderground.com/), also contributing to the smearing. We limit our attention here to May–August HCHO columns.

We oversample the OMI HCHO data over eastern Texas (99.5° – 92.5°W , 28° – 34°N) for May–August 2005–2008 by averaging individual pixels onto a $0.02^\circ \times 0.02^\circ$ ($\sim 2 \times 2 \text{ km}^2$) grid. In this procedure, the column measurement for a given pixel is assumed to apply to a circle defined by the center point of the pixel and an ‘averaging radius’ of 24 km. Previous OMI oversampling studies have used the same strategy. Fioletov *et al* (2011) chose an averaging radius of 12 km for oversampling OMI SO_2 pixels, and McLinden *et al* (2012) used 20 km and 24 km for OMI NO_2 and SO_2 pixels, respectively. We find that a 12 km or 20 km averaging radius for HCHO pixels leads to excessive noise. Our oversampling approach leads to ~ 800 OMI measurements being averaged in each $0.02^\circ \times 0.02^\circ$ grid square.

3. Results and discussion

Figure 1 (left) shows the oversampled OMI HCHO concentrations for May–August 2005–2008. Urban/industrial sources in and near Houston, Port Arthur, and Dallas/Fort Worth are clearly detected. Urban areas of Austin and San Antonio are less industrial and only marginally detected. The Houston and Port Arthur plumes are transported northward by the prevailing SSE wind. The enhancement west of Dallas/

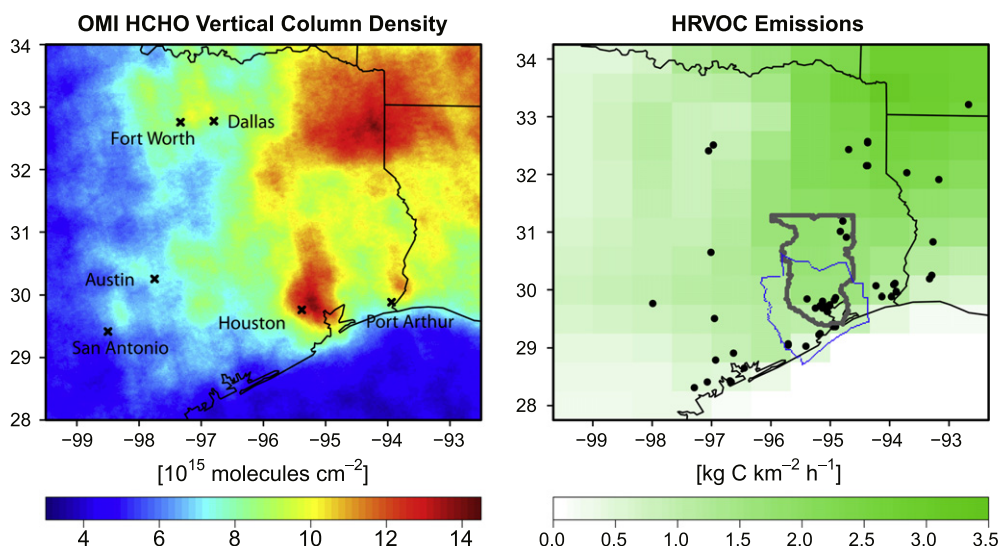


Figure 1. OMI HCHO columns and HRVOC emission inventories for eastern Texas. The left panel shows OMI HCHO columns averaged over May–August 2005–2008 and oversampled to a $0.02^\circ \times 0.02^\circ$ resolution using an averaging radius of 24 km. Crosses indicate city centers. The right panel shows the May–August 2008 biogenic isoprene emissions and the major anthropogenic HRVOC (AHRVOC, table 1) point sources (dots) with emission larger than 3 kg C h^{-1} binned on a $0.02^\circ \times 0.02^\circ$ grid. Isoprene emissions are computed with MEGAN v2.1 (Guenther *et al* 2012). AHRVOC emissions are from the 2005 National Emissions Inventory (NEI05) of the US Environmental Protection Agency (EPA) as implemented by Stuart McKeen (Brioude *et al* 2011, Kim *et al* 2011). The Houston plume outline (gray) is used in the text to estimate AHRVOC emissions from the HCHO data. The boundary of the Houston–Galveston–Brazoria urban metropolitan area (HGB) is shown as the thin blue outline.

Fort Worth can be attributed to AHRVOC emissions from the Barnett Shale, the largest onshore natural gas field in the US. The high values over Northeast Texas are due to isoprene emission as discussed below.

HCHO columns over the Houston urban area peak at $1.4 \times 10^{16} \text{ molecules cm}^{-2}$ near the Houston ship channel where major refineries and petrochemical industries emit large amounts of HRVOCs. Johansson *et al* (2014) previously reported HCHO columns in the channel of up to $2.4 \times 10^{16} \text{ molecules cm}^{-2}$ from ground-based remote sensing in May 2009. Our mean column of $9.4 \times 10^{15} \text{ molecules cm}^{-2}$ in the Houston–Galveston–Brazoria urban metropolitan area (HGB; figure 1, thin blue line) corresponds to a mean HCHO mixing ratio of 2.4 ppb for a 1.7 km deep PBL (Haman *et al* 2012). This result agrees with the mean HCHO concentration of 2.4 ppb measured in the HGB during the summer 2006 Texas Air Quality Study (TexAQS) (Gilman *et al* 2009). HGB concentrations measured during that study ranged from 1 to 20 ppb (Zhang *et al* 2013).

The right panel of figure 1 shows HRVOC emissions for eastern Texas estimated from current inventories. These include MEGAN v2.1 for biogenic isoprene (Guenther *et al* 2012) and the 2005 National Emission Inventory (NEI05) of the US Environmental Protection Agency (EPA) as implemented by Stuart McKeen (see Brioude *et al* 2011, Kim *et al* 2011). Here AHRVOCs are defined as having atmospheric lifetimes of less than 1 day against oxidation by OH. Table 1 lists the main NEI05 AHRVOCs emitted in the Houston plume area defined in figure 1 (gray line). Ethene and propene are the most important HCHO precursors, as also observed in the TexAQS campaigns (Wert *et al* 2003, Parrish *et al* 2012). Wert *et al* (2003) found from speciated VOC

samples that 78% of the HCHO production potential was from terminal alkenes including 30% from ethene, 22% from propene, 14% from isoprene, and 12% from other alkenes.

Biogenic isoprene makes a large background contribution to HCHO over eastern Texas, as seen in figure 1 and previously noted by Martin *et al* (2004). Isoprene emissions in MEGAN v2.1 are particularly high over forested Northeast Texas, explaining the high OMI HCHO columns there. Some distinction between biogenic and anthropogenic contributions to OMI HCHO can be made on the basis of correlation with surface air temperature. Isoprene emission increases exponentially with temperature (Guenther *et al* 2006), and this dependence is apparent in regional HCHO satellite data over the Southeast US (Palmer *et al* 2006). Figure 2 shows the relationships of OMI HCHO with surface air temperature over Northeast Texas and the Houston core for May–September 2006–2008. The data over Northeast Texas show a strong exponential relationship with temperature ($R^2 = 0.64$) with an argument of 0.11 K^{-1} , consistent with that expected for isoprene emission (Guenther *et al* 2006, Palmer *et al* 2006). By contrast, OMI HCHO columns over the Houston core show no significant relationship with temperature ($R^2 = 0.03$), supporting the dominant anthropogenic influence. The lack of correlation in the Houston data partly reflects a cluster of three points in figure 2 with $T > 300 \text{ K}$ and HCHO column $< 2 \times 10^{15} \text{ molecules cm}^{-2}$, but even excluding these points the relationship with temperature yields only $R^2 = 0.34$. Some correlation of HCHO with temperature would be expected even over Houston due to (1) the regional HCHO background contributed by isoprene (Wert *et al* 2003), (2) the temperature dependence of AHRVOCs oxidation, and (3) the association of high temperature with stagnation.

Table 1. NEI estimates of Houston AHRVOC emissions and HCHO yields^a.

Species	Lifetime ^b (h)	Emission ^a (kmol h ⁻¹)	Molar HCHO yield ^c	HCHO production (kmol h ⁻¹)
Ethene	2.9	16	1.6	27
Propene	0.8	6.3	1.8	12
Higher alkenes	0.6 ^d	5.3	0.6 ^d	3.2
Formaldehyde	1.6 ^e	9.4	1.0	9.4
Acetaldehyde	1.6	1.2	1.0	1.2
Other ^f	0.4 ^g	0.7	0.6 ^g	0.7
Total	—	39	—	52

^a Mean emissions for May–August 2005 from the US EPA National Emission Inventory (NEI05) implemented by Stuart McKeen (Brioude et al 2011, Kim et al 2011, <ftp://aftp.fsl.noaa.gov/divisions/taq/>) over the area of the Houston plume defined by the OMI HCHO data (figure 1, gray outline).

^b Lifetime against oxidation by OH computed using a mean OH concentration of 1.1×10^7 molecules cm⁻³ for 09:30–13:30 local time taken from Mao et al 2009. Kinetic data are from the Master Chemical Mechanism (MCM) v3.2 (Jenkin et al 1997, Saunders et al 2003, <http://mcm.leeds.ac.uk/MCM/>).

^c Prompt yield of HCHO realized within one day of initial oxidation, as computed using MCM v3.2 for oxidation by OH in the high-NO_x regime.

^d Using 1-butane as representative species.

^e Also includes photolysis, using a mean 09:30–13:30 photolysis frequency of 8.1×10^{-5} s⁻¹ computed with the Tropospheric Ultraviolet and Visible (TUV) Radiation Model (<http://cprm.acd.ucar.edu/Models/TUV/>). HCHO loss is 46% from photolysis and 54% from oxidation by OH.

^f Including dienes, glyoxal, and styrene.

^g Using 1,3-butadiene as representative species.

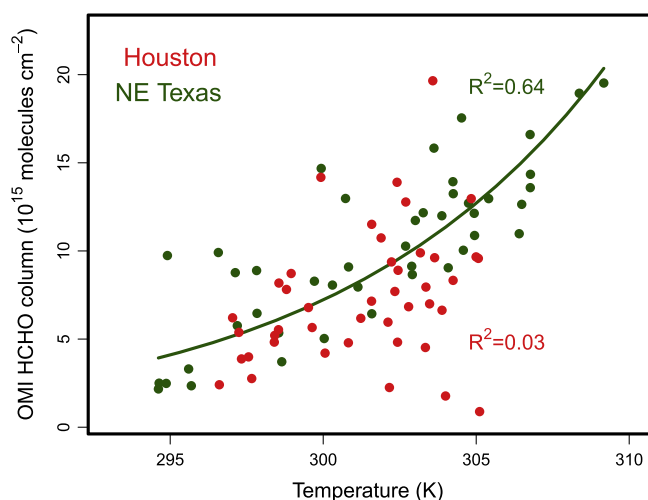


Figure 2. Relationship of OMI HCHO column with surface air temperature for the Houston urban core (95.5°–95°W, 29.5°–30°N) and Northeast Texas (95°–93.5°W, 32°–33.5°N). Temperatures are 13:00–14:00 local time values from the NASA Modern-era Retrospective Analysis for Research and Application (MERRA). Individual points are ten-day averages for May–September 2006–2008. Coefficients of determination (R^2) are shown inset. The green solid line is an exponential fit of the HCHO column (Ω) to the surface air temperature (T) over Northeast Texas as $\ln \Omega = 2.62 + 0.11T$.

A number of previous studies have used satellite HCHO data to constrain isoprene emissions by assuming a local relationship between the two from a chemical transport model (CTM) (Palmer et al 2003, Fu et al 2007, Millet et al 2008, Barkley et al 2008, Marais et al 2012) or by applying a more elaborate inversion method (Shim et al 2005, Dufour et al 2009, Stavrou et al 2009, Curci et al 2010). In regions of the world where anthropogenic HCHO is readily discernable, these approaches have also been used to constrain

AHRVOC emissions (Shim et al 2005, Fu et al 2007, Marais et al 2014b). In our case, the AHRVOC enhancement is on top of a large regional background (figure 1). We constrain AHRVOC emissions for the Houston plume area by integrating the OMI HCHO enhancement over the Houston plume as the difference between the observed HCHO column (Ω) and the regional background (Ω_0) contributed by biogenic and long-lived anthropogenic emissions. From the HCHO lifetime (τ_{HCHO}) we deduce the corresponding HCHO source S per unit time as

$$S = \frac{1}{\tau_{\text{HCHO}}} \iint (\Omega - \Omega_0) dA, \quad (1)$$

where the integral is over the area $A = 1.9 \times 10^4$ km² of the plume as defined in figure 1. This represents the total emission of AHRVOCs within the plume area weighted by their prompt yield of HCHO. We can convert this quantity to a total AHRVOC emission (E) by applying independent estimates of the fraction f_i of the total emission contributed by species i and the corresponding HCHO yield Y_i (table 1):

$$E = \frac{S}{\sum_i f_i Y_i}. \quad (2)$$

Here we estimate the regional background (Ω_0) as the HCHO column downwind of the discernible Houston plume, corresponding roughly to the green color in figure 1 ($8\text{--}10 \times 10^{15}$ molecules cm⁻²). Figure 3 shows HCHO columns averaged across the prevailing wind as a function of the distance from Houston city center. The plume decays to a regional background value at about 110 km downwind of the city center. For a mean wind speed of 3.3 m s⁻¹ (www.wunderground.com/) this corresponds to an aging time of 9.3 h, long relative to the lifetimes of ethene and propene (table 1). From the downwind asymptote of the plume we

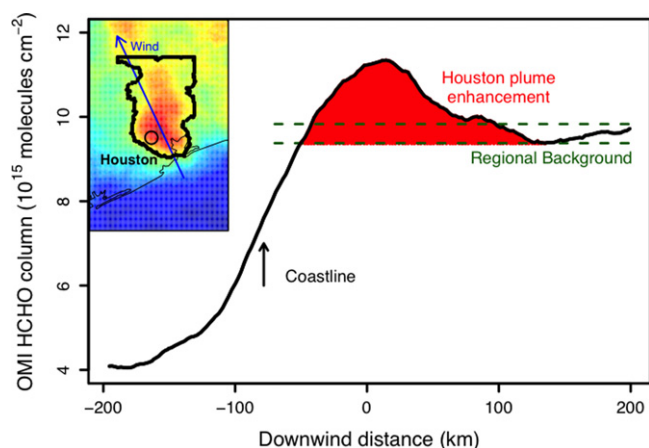


Figure 3. Cross-section of the Houston HCHO plume along the direction of the prevailing SSE wind. The inset map is an excerpt from figure 1 delineating the Houston plume (black line, same as the gray line in the right panel of figure 1). The figure shows the mean HCHO columns for May–August 2005–2008 averaged across the plume width as a function of downwind distance from the Houston city center (open circle on the map). Green dashed lines bracket the regional background (Ω_0) defined by the HCHO columns beyond the extent of the plume. The HCHO enhancement in the plume is shown as red fill.

derive a best estimate for the regional background of $\Omega_0 = 9.6 \pm 0.3 \times 10^{15}$ molecules cm^{-2} (figure 3). The actual uncertainty in the regional background is likely larger considering the fine-scale heterogeneity in isoprene emissions (Gulden, Yang Z L 2006). We therefore adopt $\Omega_0 = 9.6 \pm 0.5 \times 10^{15}$ molecules cm^{-2} as a more conservative estimate of the uncertainty. The uncertainty in the Houston plume enhancement ($\Omega - \Omega_0$) is largely defined by the uncertainty in Ω_0 , considering that any systematic errors in the retrieval would likely be canceled in computing the difference between Ω and Ω_0 . We thus obtain a total HCHO column enhancement integrated over the plume of 400 ± 180 kmol (red area in figure 3).

Loss of HCHO is by photolysis and oxidation by OH. From table 1, we estimate τ_{HCHO} to be 1.6 h. Photolysis accounts for half of total HCHO loss and is relatively well constrained. Loss by reaction with OH is not as well constrained because of uncertainty in OH concentrations. Here we adopted a mean OH concentration of 1.1×10^7 molecules cm^{-3} at 09:30–13:30 local time from measurements in downtown Houston (Mao *et al* 2009) and estimate the overall uncertainty in τ_{HCHO} to be 30%. The resulting anthropogenic HCHO source S over the area of the plume is 250 ± 140 kmol HCHO h^{-1} , propagating in quadrature our estimated uncertainty in τ_{HCHO} .

Combining this result with the data on f_i and Y_i in table 1, we deduce a total AHRVOC emission E for the HGB of 190 ± 100 kmol h^{-1} , which can be compared to the NEI05 estimate of 39 kmol h^{-1} from table 1. The OMI observations thus suggest that AHRVOC emissions in the Houston plume area are underestimated by a factor of 4.8 ± 2.7 in the NEI05 inventory for 2005–2008. This is consistent with previous studies pointing to a large underestimate of alkene emissions

in the HGB (e.g., Wert *et al* 2003, de Gouw *et al* 2009, Parrish *et al* 2009, Mellqvist *et al* 2010). Our estimate of the HCHO source in the Houston plume is consistent with the estimate of 240 ± 90 kmol HCHO h^{-1} from Parrish *et al* (2012) computed using an improved alkene inventory (Kim *et al* 2011) with updated ethene and propene emission factors from petrochemical facilities (Mellqvist *et al* 2010).

Previous analyses of HCHO data in Houston have reached contradictory conclusions on whether most of the HCHO is primary, i.e., directly emitted (Rappengluck *et al* 2010, Buzcu Guven and Olaguer 2011, Olaguer 2013, Olaguer *et al* 2013, Johansson *et al* 2014) or secondary, i.e., produced within the plume from alkene oxidation (Friedfeld *et al* 2002, Wert *et al* 2003, Parrish *et al* 2012, Zhang *et al* 2013). The distinction is important because primary HCHO would accumulate at night and photolyze in early morning, providing a source of radicals to initiate ozone formation. Our inability to detect the Houston urban plume in winter from the OMI data (see above) argues against a major primary source of HCHO. We attempted to constrain the speciation of AHRVOCs by using the shape of the OMI plume in figure 3 and a simple constant-wind model, as primary HCHO would decay closer to the core. We were unsuccessful, partly because of the complexity arising from primary emissions at night and in early morning when the HCHO lifetime is long.

We see from figures 1 and 3 that the anthropogenic HCHO enhancements in the Houston plume and elsewhere are on top of a larger regional background (Ω_0). This background is dominantly from biogenic isoprene. For the Houston plume area in figure 3, the 24 h average isoprene emission calculated by MEGAN in May–August is 95 kmol h^{-1} . Assuming a HCHO molar yield of 2.3 from isoprene oxidation (Millet *et al* 2006), this yields a HCHO production rate of 220 kmol h^{-1} , comparable in magnitude to the anthropogenic source.

Observations from the TexAQS aircraft campaigns in 2000 and 2006 documented a decrease of AHRVOC emissions from the HGB over that period. Gilman *et al* (2009) reported 56% and 51% decreases in ethene and propene median concentrations, respectively; Washenfelder *et al* (2010) found emission decreases in the Houston ship channel of 41% for ethene and 8% for propene from 1999 to 2006. Presently the useful OMI HCHO record is limited to 2005–2008; data after 2008 are too noisy for trend analysis because of the row anomaly. De Smedt *et al* (2010) used data from the GOME and SCIAMACHY satellite instruments to infer global 1997–2009 trends in HCHO, but we find that the pixel resolution of these instruments is too coarse for detection of the Houston plume. Post-2008 OMI data are expected to be corrected in a future product (González Abad *et al* 2014), which will then allow analysis of AHRVOC trends as well as examination of AHRVOC emissions associated with the large increase in oil/gas exploration across the US over the past five years.

4. Conclusions

We have shown that multi-year oversampling of summertime OMI HCHO satellite data enables detection of HCHO enhancements from large US urban/industrial sources of anthropogenic highly reactive volatile organic compounds (AHRVOCs). The enhancement in the Houston urban plume is sufficiently extensive to allow quantitative interpretation in terms of AHRVOC emissions. Our resulting estimate of AHRVOC emissions for Houston is 4.8 ± 2.7 times higher than the US EPA inventory and consistent with previous field estimates that identified large ethene and propene emissions from the petrochemical industry. The lack of detectable OMI HCHO enhancements in winter suggests that anthropogenic HCHO is mainly produced by photochemical oxidation of alkenes rather than directly emitted.

Acknowledgements

This work was supported by the NASA Aura Science Team and Air Quality Applied Sciences Team. The authors thank Barry Lefer and James Flynn at the University of Houston and Xiong Liu at the Harvard-Smithsonian Center for Astrophysics for their help. We thank two anonymous reviewers who provided thorough and thoughtful comments.

References

- Barkley M P, Palmer P I, Kuhn U, Kesselmeier J, Chance K, Kurosu T P, Martin R, Helmig V and Guenther A 2008 Net ecosystem fluxes of isoprene over tropical South America inferred from Global Ozone Monitoring Experiment (GOME) observations of HCHO columns *J. Geophys. Res.* **113** D20304
- Boeke N L *et al* 2011 Formaldehyde columns from the Ozone monitoring instrument: urban versus background levels and evaluation using aircraft data and a global model *J. Geophys. Res.* **116** D05303
- Brioude J *et al* 2011 Top-down estimate of anthropogenic emission inventories and their interannual variability in Houston using a mesoscale inverse modeling technique *J. Geophys. Res.* **116** D20305
- Buzcu Guven B and Olaguer E P 2011 Ambient formaldehyde source attribution in Houston during TexAQS II and TRAMP *Atmos. Environ.* **45** 4272–80
- Chance K, Palmer P I, Spurr R J D, Martin R V, Kurosu T P and Jacob D J 2000 Satellite observations of formaldehyde over North America from GOME *Geophys. Res. Lett.* **27** 3461–4
- Curci G, Palmer P I, Kurosu T P, Chance K and Visconti G 2010 Estimating European volatile organic compound emissions using satellite observations of formaldehyde from the Ozone monitoring instrument *Atmos. Chem. Phys.* **10** 11501–17
- de Foy B, Krotkov N A, Bei N, Herndon S C, Huey L G, Martínez A-P, Ruiz-Suárez L G, Wood E C, Zavala M and Molina L T 2009 Hit from both sides: tracking industrial and volcanic plumes in Mexico City with surface measurements and OMI SO₂ retrievals during the MILAGRO field campaign *Atmos. Chem. Phys.* **9** 9599–617
- de Gouw J A, Johansson J, Mellqvist J, Samuelsson J, Offerle B and Rappengluck B 2009 Airborne measurements of ethene from industrial sources using laser photo-acoustic spectroscopy *Environ. Sci. Technol.* **43** 2437–42
- De Smedt I, Stavrakou T, Müller J-F, van der A R J and Van Roozendaal M 2010 Trend detection in satellite observations of formaldehyde tropospheric columns *Geophys. Res. Lett.* **37** L18808
- Dufour G, Wittrock F, Camredon M, Beekmann M, Richter A, Aumont B and Burrows J P 2009 SCIAMACHY formaldehyde observations: constraint for isoprene emission estimates over Europe? *Atmos. Chem. Phys.* **9** 1647–64
- Fioletov V E, McLinden C A, Krotkov N, Moran M D and Yang K 2011 Estimation of SO₂ emissions using OMI retrievals *Geophys. Res. Lett.* **38** L21811
- Friedfeld S, Fraser M, Ensor K, Tribble S, Rehle D, Leleux D and Tittel F 2002 Statistical analysis of primary and secondary atmospheric formaldehyde *Atmos. Environ.* **36** 4767–75
- Fu T-M, Jacob D J, Palmer P I, Chance K, Wang Y X, Barletta B, Blake D R, Stanton J C and Pilling M J 2007 Space-based formaldehyde measurements as constraints on volatile organic compound emissions in east and south Asia and implications for ozone *J. Geophys. Res.* **112** D06312
- Gilman J B *et al* 2009 Measurements of volatile organic compounds during the 2006 TexAQS/GoMACCS campaign: industrial influences, regional characteristics, and diurnal dependencies of the OH reactivity *J. Geophys. Res.* **114** D00F06
- Gilman J B, Lerner B M, Kuster W C and de Gouw J A 2013 Source signature of volatile organic compounds from oil and natural gas operations in Northeastern Colorado *Environ. Sci. Technol.* **47** 1297–305
- González Abad G, Liu X, Chance K, Wang H, Kurosu T P and Suleiman R 2014 Updated SAO OMI formaldehyde retrieval *Atmos. Meas. Tech. Discuss.* **7** 1–31
- Guenther A, Karl T, Harley P, Wiedinmyer C, Palmer P I and Geron C 2006 Estimates of global terrestrial isoprene emissions using MEGAN (model of emissions of gases and aerosols from nature) *Atmos. Chem. Phys.* **6** 3181–210
- Guenther A B, Jiang X, Heald C L, Sakulyanontvittaya T, Duhl T, Emmons L K and Wang X 2012 The model of emissions of gases and aerosols from nature version 2.1 (MEGAN2.1): an extended and updated framework for modeling biogenic emissions *Geosci. Model Dev.* **5** 1471–92
- Gulden L E and Yang Z L 2006 Development of species-based, regional emission capacities for simulation of biogenic volatile organic compound emissions in land-surface models: an example from Texas, USA *Atmos. Environ.* **40** 1464–79
- Haman C L, Lefer B and Morris G A 2012 Seasonal variability in the diurnal evolution of the boundary layer in a near-coastal urban environment *J. Atmos. Oceanic Technol.* **29** 697–710
- Jenkin M E, Saunders S M and Pilling M J 1997 The tropospheric degradation of volatile organic compounds: a protocol for mechanism development *Atmos. Environ.* **31** 81–104
- Johansson J K E, Mellqvist J, Samuelsson J, Offerle B, Moldanova J, Rappengluck B, Lefer B and Flynn J 2014 Quantitative measurements and modeling of industrial formaldehyde emissions in the Greater Houston area during campaigns in 2009 and 2011 *J. Geophys. Res.* **119** 4303–22
- Kim S-W *et al* 2011 Evaluations of NO_x and highly reactive VOC emission inventories in Texas and their implications for ozone plume simulations during the Texas air quality study 2006 *Atmos. Chem. Phys.* **11** 11361–86
- Levelt P F, van den Oord G H J, Dobber M R, Malkki A, Visser H, de Vries J, Stammes P, Lundell J O V and Saari H 2006 The Ozone monitoring instrument *IEEE Trans. Geo. Rem. Sens.* **44** 1093–101
- Lin Y C, Schwab J J, Demerjian K L, Bae M-S, Chen W-N, Sun Y, Zhang Q, Hung H-M and Perry J 2012 Summertime formaldehyde observations in New York City: Ambient levels, sources and its contribution to HO_x radicals *J. Geophys. Res.* **117** D08305
- Lu Z, Streets D G, de Foy B and Krotkov N A 2013 Ozone Monitoring Instrument observations of interannual increases in

- SO₂ emissions from Indian coal-fired power plants during 2005–2012 *Environ. Sci. Technol.* **47** 13993–14000
- Mao J et al 2009 Atmospheric oxidation capacity in the summer of Houston 2006: comparison with summer measurements in other metropolitan studies *Atmos. Environ.* **44** 4107–15
- Marais E A et al 2012 Isoprene emissions in Africa inferred from OMI observations of formaldehyde columns *Atmos. Chem. Phys.* **12** 6219–35
- Marais E A, Jacob D J, Guenther A, Chance K, Kurosu T P, Murphy J G, Reeves C E and Pye H O T 2014b Improved model of isoprene emissions in Africa using Ozone Monitoring Instrument (OMI) satellite observations of formaldehyde: implications for oxidants and particulate matter *Atmos. Chem. Phys.* **14** 7693–703
- Marais E A, Jacob D J, Wecht K, Lerot C, Kurosu T P and Chance K 2014a Anthropogenic emissions in Nigeria and air quality implications: a view from space *Atmos. Environ.* **99** 32–40
- Martin R V, Parrish D D, Ryerson T B, Nicks D K Jr, Chance K, Kurosu T P, Jacob D J, Sturges E D, Fried A and Wert B P 2004 Evaluation of GOME satellite measurements of tropospheric NO₂ and HCHO using regional data from aircraft campaigns in the southeastern United States *J. Geophys. Res.* **109** D24307
- McLinden C A, Fioletov V, Boersma K F, Krotkov N, Sioris C E, Veefkind J P and Yang K 2012 Air quality over the Canadian oil sands: A first assessment using satellite observations *Geophys. Res. Lett.* **39** L04804
- Mellqvist J, Samuelsson J, Johansson J, Rivera C, Lefer B, Alvarez S and Jolly J 2010 Measurements of industrial emissions of alkenes in Texas using the solar occultation flux method *J. Geophys. Res.* **115** D00F17
- Millet D B et al 2006 Formaldehyde distribution over North America: implications for satellite retrievals of formaldehyde columns and isoprene emission *J. Geophys. Res.* **111** D24S02
- Millet D B, Jacob D J, Boersma K F, Fu T M, Kurosu T P, Chance K, Heald C L and Guenther A 2008 Spatial distribution of isoprene emissions from North America derived from formaldehyde column measurements by the OMI satellite sensor *J. Geophys. Res.* **113** D02307
- Olaguer E P 2013 Application of an adjoint neighborhood-scale chemistry transport model to the attribution of primary formaldehyde at Lynchburg Ferry during TexAQS II *J. Geophys. Res. Atmos.* **118** 4936–46
- Olaguer E P, Herndon S C, Buzcu-Guven B, Kolb C E, Brown M J and Cuclis A E 2013 Attribution of primary formaldehyde and sulfur dioxide at Texas City during SHARP/formaldehyde and olefins from large industrial releases (FLAIR) using an adjoint chemistry transport model *J. Geophys. Res. Atmos.* **118** 11317–26
- Palmer P I et al 2001 Air mass factor formulation for spectroscopic measurements from satellites: application to formaldehyde retrievals from the global ozone monitoring experiment *J. Geophys. Res.* **106** 14539–50
- Palmer P I et al 2006 Quantifying the seasonal and interannual variability of North American isoprene emissions using satellite observations of the formaldehyde column *J. Geophys. Res.* **111** D12315
- Palmer P I, Jacob D J, Fiore A M, Martin R V, Chance K and Kurosu T P 2003 Mapping isoprene emissions over North America using formaldehyde column observations from space *J. Geophys. Res.* **108** 4180
- Parrish D D et al 2009 Overview of the second Texas Air Quality Study (TexAQS II) and the Gulf of Mexico Atmospheric Composition and Climate Study (GoMACCS) *J. Geophys. Res.* **114** D00F13
- Parrish D D et al 2012 Primary and secondary sources of formaldehyde in urban atmospheres: Houston Texas region *Atmos. Chem. Phys.* **12** 3273–88
- Rappengluck B, Dasgupta P K, Leuchner M, Li Q and Luke W 2010 Formaldehyde and its relation to CO, PAN, and SO₂ in the Houston–Galveston airshed *Atmos. Chem. Phys.* **10** 2413–24
- Ryerson T B et al 2003 Effect of petrochemical industrial emissions of reactive alkenes and NO_x on tropospheric ozone formation in Houston, Texas *J. Geophys. Res.* **108** 4249
- Saunders S M, Jenkin M E, Derwent R G and Pilling M J 2003 Protocol for the development of the Master Chemical Mechanism, MCM v3 (Part A): tropospheric degradation of non-aromatic volatile organic compounds *Atmos. Chem. Phys.* **3** 161–80
- Shim C, Wang Y, Choi Y, Palmer P I, Abbot D S and Chance K 2005 Constraining global isoprene emissions with Global Ozone Monitoring Experiment (GOME) formaldehyde column measurements *J. Geophys. Res.* **110** D24301
- Spurr R J D, Kurosu T P and Chance K V 2001 A linearized discrete ordinate radiative transfer model for atmospheric remote sensing retrieval *J. Quant. Spectrosc. Radiat. Transfer* **68** 689–735
- Stavrakou T, Müller J-F, De Smedt I, Van Roozendael M, van der Werf G R, Giglio L and Guenther A 2009 Global emissions of non-methane hydrocarbons deduced from SCIAMACHY formaldehyde columns through 2003–2006 *Atmos. Chem. Phys.* **9** 3663–79
- Washenfelder R A et al 2010 Characterization of NO_x, SO₂, ethene, and propene from industrial emission sources in Houston, Texas *J. Geophys. Res.* **115** D16311
- Wert B P et al 2003 Signatures of terminal alkene oxidation in airborne formaldehyde measurements during TexAQS 2000 *J. Geophys. Res.* **108** 4104
- Zhang H, Li J, Ying Q, Guven B B and Olaguer E P 2013 Source apportionment of formaldehyde during TexAQS 2006 using a source-oriented chemical transport model *J. Geophys. Res. Atmos.* **118** 1525–35
- Zhang L, Jacob D J, Downey N V, Wood D A, Blewitt D, Carouge C C, van Donkelaar A, Jones D B A, Murray L T and Wang Y 2011 Improved estimate of the policy-relevant background ozone in the United States using the GEOS-Chem global model with 1/2° × 2/3° horizontal resolution over North America *Atmos. Environ.* **45** 6769–76
- Zheng J et al 2013 Measurements of formaldehyde at the US–Mexico border during the Cal-Mex 2010 *Air Quality Study Atmos. Environ.* **70** 513–20